Society For Biomaterials

Polylactide nanofibers with hydroxyapatite as growth substrates for osteoblast-like cells

Katarina Novotna,[1] Martina Zajdlova,[1] Tomas Suchy,[2] Daniel Hadraba,[1] Frantisek Lopot,[3] Margit Zaloudkova,[2] Timothy E.L. Douglas,[4] Marcela Munzarova,[5*] Martina Juklickova,[5] Denisa Stranska,[5] Dana Kubies,[6] David Schaubroeck,[7] Sebastian Wille,[8] Lieve Balcaen,[9] Marketa Jarosova,[10] Halyna Kozak,[10] Alexander Kromka,[10] Zdenek Svindrych,[1] Vera Lisa,[1] Karel Balik,[2] Lucie Bacakova[1]

[1]Department of Biomaterials and Tissue Engineering, Institute of Physiology, Academy of Sciences of the Czech Republic, Videnska, 1083, 14220 Prague 4, Czech Republic
[2]Department of Composites and Carbon Materials, Institute of Rock Structure and Mechanics, Academy of Sciences of the Czech Republic, V Holesovickach 41, 18209 Prague 8, Czech Republic
[3]Faculty of Mechanical Engineering of Czech Technical University in Prague, Technicka 4, 16607 Prague 6, and Laboratory of Extreme Loading, Dept. Anatomy and Biomechanics, Charles University in Prague, Jose Martiho 31, 162 52 Prague 6, Czech Republic
[4]Polymer Chemistry and Biomaterials (PBM) Group, Department of Organic Chemistry, Ghent University, Campus Sterre, Krijgslaan 281 S4, 9000 Gent, Belgium
[5]ELMARCO, Svarovska 621, 46010 Liberec 10, Czech Republic
[6]Department of Biomaterials and Bioanalogous Polymer Systems, Institute of Macromolecular Chemistry, Academy of Sciences of the Czech Republic, Heyrovsky Sq. 2, 16206 Prague 6, Czech Republic
[7]Center for Microsystems Technology (CMST), ELIS, imec, Technologiepark 914A, 9052 Gent, Belgium
[8]Functional Nanomaterials, Institute for Materials Science, Faculty of Engineering, Christian-Albrechts-University Kiel, Kaiserstr. 2, 24143 Kiel, Germany
[9]Department of Analytical Chemistry, Ghent University, Krijgslaan 281 S12, 9000 Gent, Belgium
[10]Institute of Physics, Academy of Sciences of the Czech Republic, Cukrovarnicka 10, 16200 Prague 6, Czech Republic

Received 2 July 2013; revised 21 October 2013; accepted 9 December 2013
Published online 00 Month 2013 in Wiley Online Library (wileyonlinelibrary.com). DOI: 10.1002/jbm.a.35061

Abstract: Various types of nanofibers are increasingly used in tissue engineering, mainly for their ability to mimic the architecture of tissue at the nanoscale. We evaluated the adhesion, growth, viability, and differentiation of human osteoblast-like MG 63 cells on polylactide (PLA) nanofibers prepared by needle-less electrospinning and loaded with 5 or 15 wt % of hydroxyapatite (HA) nanoparticles. On day 7 after seeding, the cell number was the highest on samples with 15 wt % of HA. This result was confirmed by the XTT test, especially after dynamic cultivation, when the number of metabolically active cells on these samples was even higher than on control polystyrene. Staining with a live/dead kit showed that the viability of cells on all nanofibrous scaffolds was very high and comparable to that on control polystyrene dishes. An enzyme-linked immunosorbent assay revealed that the concentration of osteocalcin was also higher in cells on samples with 15 wt % of HA. There was no immune activation of cells (measured by production of TNF-alpha), associated with the incorporation of HA. Moreover, the addition of HA suppressed the creep behavior of the scaffolds in their dry state. Thus, nanofibrous PLA scaffolds have potential for bone tissue engineering, particularly those with 15 wt % of HA. © 2013 Wiley Periodicals, Inc. J Biomed Mater Res Part A: 00A: 000–000, 2013.

Key Words: electrospinning, nanofibers, polylactide, hydroxyapatite, tissue engineering

How to cite this article: Novotna K, Zajdlova M, Suchy T, Hadraba D, Lopot F, Zaloudkova M, Douglas TEL, Munzarova M, Juklickova M, Stranska D, Kubies D, Schaubroeck D, Wille S, Balcaen L, Jarosova M, Kozak H, Kromka A, Svindrych Z, Lisa V, Balik K, Bacakova L. 2013. Polylactide nanofibers with hydroxyapatite as growth substrates for osteoblast-like cells. J Biomed Mater Res Part A 2013:00A:000–000.

Additional Supporting Information may be found in the online version of this article.
*Present address: NANOVIA, Podkrusnohorska 271, 43603 Litvinov-Chuderin, Czech Republic
Correspondence to: Lucie Bacakova, Associate Professor, Department of Biomaterials and Tissue Engineering, Institute of Physiology, Academy of Sciences of the Czech Republic, Videnska 1083, CZ-14220 Prague 4-Krc, Czech Republic; e-mail: lucy@biomed.cas.cz
Contract grant sponsor: Grant Agency of the Czech Republic; contract grant number: 106/09/1000; P108/10/1106
Contract grant sponsor: Research Foundation Flanders (FWO), postdoctoral research fellowship to T.E.L.D.

INTRODUCTION

The development of nanofibrous scaffolds has opened new possibilities in various tissue engineering applications thanks to the nanofibers' advantageous properties, such as high surface area, macroporosity, and combined micro- and nanoscale roughness, which closely imitate natural extracellular matrix and promote cell adhesion and proliferation. Scaffolds with nanofibrous architecture have been proven to promote protein adsorption, subsequent attachment of osteoblasts, their differentiation and biomineralization.[1] Nanofibers can be prepared by several techniques, but electrospinning is one of the most widely used due to its effectiveness and simplicity.[2] Electrospinning produces randomly oriented fibers with various diameters usually ranging from tens of nanometers to one micrometer or even thicker, and this organization seems to be very favorable for cells.[3]

Although the nanofibers themselves present a good support for cell growth, they have been often modified with bioactive particles to improve their mechanical properties and/or bioactivity. For bone tissue engineering, the most common additions to polymer nanofibers are hydroxyapatite (HA) and tricalcium phosphates.[4,5] In a recently published study, the addition of diamond nanoparticles to PLGA nanofibrous membranes was tested. These composite scaffolds showed improved mechanical resistance and provided a good support for bone cell adhesion and growth.[6]

HA, being a promising material for bone tissue engineering, has been frequently tested either alone[7] or as a part of a composite.[8] It is similar to the mineral which occurs naturally in bone, it is biocompatible, it has appropriate mechanical stability, and it has been proved to be osteoconductive and to promote one formation.[9] Especially nanosized HA particles (e.g., in the form of sintered compacts) have promoted osteoblast adhesion, proliferation and differentiation, and seem to be more beneficial in bone tissue engineering than conventional HA, that is, with grains greater than 100 nm.[10]

Composites constructed from polymers and HA combine advantages of both material types. While HA improves osteoinduction and provides mechanical reinforcement, biodegradability of polymers allows ingrowth of the surrounding tissue. Following the example of bone as a complex tissue consisting of organic collagen fibers and inorganic mineral apatite, we have constructed polylactide nanofibrous scaffolds with two concentrations of HA nanoparticles by a needle-less electrospinning technique. Similar composite materials have been also constructed in earlier studies.[11–13] However, this study provides an intensive and systematic investigation of morphological, physical and chemical properties of these scaffolds, and their correlation with the behavior of human bone-derived and rat macrophage-like cells in cultures on these scaffolds.

MATERIALS AND METHODS

Preparation of the scaffolds

Poly(L-lactide) (PLA, Ingeo™ Biopolymer 4032D) was a product of NatureWorks, Minnetonka, Minnesota, USA. Its molecular masses were $M_w = 124{,}000$ g/mol and $M_n = 48{,}000$ g/mol, as determined by size exclusion chromatography.[14] For the electrospinning process, 7 wt % solution of PLA in a mixture of chloroform, dichloroethane, and ethyl acetate was used. The polymer solution was made to be electrically conductive with tetraethylammoniumbromide, which was first dissolved in dimethylformamide at a concentration of 3 wt %, after which 3 g of this solution was added to 100 g of the PLA solution. To prepare composite scaffolds of PLA with HA (BABI-HAP-N100, average particle size 50–150 nm, Ca:P ratio 1.67, Berkeley Advanced Biomaterials, San Leandro, CA), two concentrations of HA were added to the prepared PLA solution before electrospinning. After addition of HA particles, the suspension was intensively vortexed and sonicated for 2 min (Bandelin Sonorex, Heidolph) in order to minimize clustering of the particles. The content of HA in the final dry scaffolds was calculated to be 5 wt % or 15 wt % relative to the polymer. Nanofibers were prepared by a needleless electrospinning technology using a Nanospider™ unit (NS Lab 500, Elmarco, Liberec, Czech Republic). Process conditions were: electrode distance: 180 mm; voltage: 60 kV, −10 kV; spinning electrode rotation speed: 4 rpm; relative humidity: 25–30% and room temperature. The weight of the prepared nanofibers per unit area was approximately 5 g/m^2.

Characterization of the scaffolds

The PLA scaffolds were characterized by scanning electron microscopy (SEM, Quanta 450 Microscope, FEI, USA) in high vacuum mode. The fiber diameters were measured by image analysis using NIS-Elements AR software, version 2.30 (Laboratory Imaging, Czech Republic). The measurement of the thickness of nanofibrous membranes was also performed (Mitutoyo Absolute, Mitutoyo Measuring Instruments, China). The nanofiber layer was immersed into liquid nitrogen and was quickly cut off with a razor blade. Images were made using a Quanta 200 (FEI supplier, CZ). The fibril morphology was evaluated by atomic force microscopy (AFM) using an alpha 300 A, WITec (Germany), in AC mode with phase imaging. In order to visualize HA nanoparticles, transmission electron microscopy (TEM) was performed.[6] The presence of HA nanoparticles in PLA scaffolds was verified by energy dispersive X-Ray spectroscopy (EDS). The concentrations of elemental Ca and P and the Ca/P molar ratio were determined by inductively coupled plasma optical emission spectroscopy (ICP-OES).[15] The determination of the real content of the HA incorporated into PLA scaffolds was performed by thermal gravimetric analysis (TGA) conducted on a Perkin Elmer TGA 7 Thermal Analyzer with Pyris 1 software in a heating range from 40 to 800°C under air (heating rate 10°C/min). The functional groups on the PLA surface were studied by attenuated total reflection Fourier transform infrared (ATR-FTIR) spectroscopy (Thermo Nicolet 8700 spectrometer with a KBr beamsplitter and a MCT detector cooled by liquid nitrogen).

For mechanical testing, rectangular strips with initial length between 30 and 70 mm and width from 12 to 18 mm were prepared. The thickness was not monitored. The mechanical behavior of PLA and PLA with HA (5 and 15 wt %) in the dry and wet states was studied using a μTester tensile instrument and the optical system. The μTester

tensile instrument setup variability enables detection of generated nominal force ranging from units to hundreds of Newtons with sensitivities of 0.04 *N*, 0.1 *N*, respectively. The optical system setup consists of the microscope Samsung SZX 12, obj. DS PLFL 1.2x, which is connected to a high performance digital 12 bit CCD camera (PCO Sensicam and ImageJ). The rectangular strips of the samples were dissected, the ends were sealed with adhesive tape, mounted into the grips and two 0.5 mm notches were made in the middle. The testing protocol consisted of an ultimate tensile strength test of the samples ($n = 12$). In addition, each sample was marked with two dots and deformed at 1 mm/s. Movement was recorded by the optical system at 7.82 fps. At the end, the detected force, time and elongation were analyzed to determine mechanical properties.

As the samples were relatively thin in comparison to their length and width, the thickness of samples was considered constant, and therefore the material parameters were set relative to the width and length of the samples. In an effort to distinguish this parameter from commonly used stiffness and stress, an equivalent stiffness and equivalent stress (force) was utilized. The abovementioned approach is legitimate because the method compares only samples from the same fundamental material of the same thickness. The detected creep was modeled as a "discontinuous function" composed from two linear lines, increasing and constant. The intersection of the lines defines the creep limit in terms of elongation.

Cell culture conditions

Prior to cell seeding, the materials were washed in distilled and deionized water for 3 days to avoid any possible effect of the residue substances from the nanofiber preparation on the cell behavior. These samples were subjected to additional analysis by SEM, EDS, ICP-OES, and TGA. The membranes were fixed in CellCrown inserts (Scaffdex, diameter 1.1 cm), sterilized in 70% ethanol for 1 h, and rinsed in distilled water and in the relevant cell culture medium (see below). Samples were inserted into polystyrene 12-well cell culture plates (TPP, Trasadingen, Switzerland) and seeded with human osteoblast-like MG 63 cells (European Collection of Cell Cultures, Salisbury, UK) in Dulbecco's modified Eagle's minimum essential medium (DMEM; Sigma, USA, Cat. No. D5648) or with mouse macrophage-like RAW 264.7 cells (American Type Culture Collection, Manassas, VA) in RPMI-1640 Medium (Sigma, USA, Cat. No. R 6504), both supplemented with 10% fetal bovine serum (Sebak GmbH, Aidenbach, Germany) and gentamicin (40 μg/mL, LEK, Ljubljana, Slovenia). Each well contained 60,000 cells and 2 mL medium. Cells were cultured in a humidified atmosphere containing 5% CO_2 in the air. The polystyrene culture dish was used as a reference material.

Evaluation of the cell growth and viability

On days 1, 3, and 7 after seeding the cells were rinsed with phosphate-buffered saline (PBS; Sigma, USA), detached from the materials by a trypsin-EDTA solution (Sigma, USA, Cat. No. T4174) and counted in a Bürker haemocytometer. Cells were also cultivated for 7 days under dynamic conditions using a Mini orbital Shaker SSM1 (Stuart). Speed was set to 50 rpm during the first 24 h and increased to 110 rpm for the rest of the cultivation period (6 days). Control cells were cultured under static conditions. The cell proliferation and viability was evaluated using cell proliferation kit II (XTT, Roche, Cat. No. 11465015 001). Absorbances were measured using ELISA Microplate Reader Versa Max (Molecular Devices, Sunnyvale, CA). On day 7, the viability of the cells was evaluated using a live/dead viability/cytotoxicity kit for mammalian cells (Invitrogen, Molecular Probes, USA, Cat. No. L3224).[6]

Evaluation of the osteogenic cell differentiation

On day 7 after seeding, the presence and spatial arrangement of osteocalcin, that is, an important marker of osteogenic differentiation, were visualized in MG 63 cells using immunocytochemical staining. The concentration of osteocalcin was measured per mg of protein in cell homogenates using an enzyme-linked immunosorbent assay (ELISA).[16]

Evaluation of the potential cell immune activation

The concentration of TNF-α was measured in cell culture media after cultivation of RAW 264.7 cells on the tested materials and on control PS dishes for 7 days using Mouse TNF-α ELISA Kit (Thermo Scientific, Rockford, IL, Cat. No. 1347.4 EMTNFA). As a positive control for TNF-α production, lipopolysaccharide (LPS; Sigma, USA, Cat. No. L 2654, concentration 0.5 ng/mL) stimulation of cells was used for the last 24 h of cultivation. The concentrations of TNF-α were expressed in pg per 100,000 cells.[6]

Statistical analysis

For fiber size measurement, the statistical analysis was carried out using STATGRAPHICS Centurion XV, StatPoint, USA. Due to the non-normality of assessed data and due to violation of the homoscedasticity assumption, the statistically significant differences were finally checked by the Kruskal-Wallis and the Mann-Whitney post hoc tests ($p = 0.01$, $p = 0.05$). The mean values are presented as median ± interquartile range (IQR). Biological results were expressed as means ± S.E.M (Standard Error of Mean). Multiple comparison procedures were performed by the one-way analysis of variance (ANOVA), Student-Newman-Keuls Method. p values equal to or less than 0.05 were considered significant. If only two experimental groups were compared, the *t*-test was utilized.

RESULTS

Morphology of the scaffolds

The fiber diameter distribution is illustrated using a Box-and-Whiskers plot (Fig. 1). In pure PLA nanofibrous layers, the diameter of fibers was in the range of 160–340 nm. The addition of 5 wt % of HA had a statistically significant influence ($p \leq 0.01$) on increase in fiber diameter, which was in the range of 287–545 nm. Further statistically significant differences ($p \leq 0.01$) were found when comparing pure PLA fibers and PLA fibers with 15 wt % of HA (with diameters in the range of 242–729 nm). Representative SEM

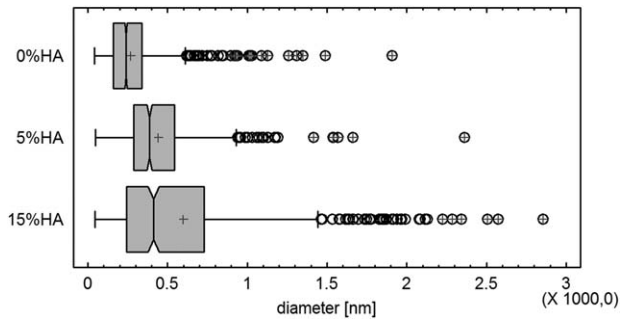

FIGURE 1. Box-and-Whiskers plot of fiber diameter ($n = 850$). Boxes indicate interquartile range (IQR), whiskers 10–90 percentile range, outside dots indicate values more than 1.5 times the IQR above or below the boxes and points more than three times the IQR above or below the box are indicated by point symbols with superimposed plus signs. A vertical line is drawn at the median. A plus sign inside the box indicates the arithmetical average. The notches for median show median confidence intervals at the 95% confidence level.

photographs are shown in Figure 2. The 3-day incubation in distilled and deionized water apparently did not affect the morphology of the scaffolds (see Supporting Information). The thickness of the nanofibrous membranes increased with increasing HA content, being 18, 31, and 33 μm in PLA membranes with 0, 5, and 15 wt % of HA, respectively. The cross sectional images of nanofibers are presented in Figure 3. The phase AFM images show that fibers in the 15 wt % HA group appear to be "rougher" than those in the pure PLA, which may be caused by the presence of hard ceramic nanoparticles or nanoparticle aggregates directly under or on the surface (Fig. 4). TEM images (Fig. 5) confirmed that HA particles were contained in the fibers (or attached to the fibers) either as single particles or in clusters. The distribution of the HA particles was relatively inhomogeneous, with some fibers containing a large amount of HA, while others were almost HA-free.

Chemical composition of the scaffolds

EDS confirmed the presence of P and Ca, and thus HA. Signals for Ca and P were absent in 0 wt %, higher in 5 wt % and higher still in 15 wt % of HA samples (Fig. 6). A similar picture was obtained when the samples were washed in distilled and deionized water for 3 days. This washing led to a decrease of Ca and P elemental fractions, but with the exception of the Ca fraction in samples with 5 wt % of HA, these differences were not statistically significant (see Supporting Information). EDS-based elemental mapping of P, Ca, C and O revealed that the most intense signals for Ca and P were observed in spherical regions of diameter approximately 10 μm or less entangled in the nanofiber network of 5 wt % and 15 wt % of HA samples (Fig. 7). More spherical regions are present in the 15 wt % than in the 5 wt % of HA sample.

For each sample, one EDS spot analysis was performed on three different spherical particles (Fig. 8). Atomic Ca/P ratios of 1.10 ± 0.2 and 1.50 ± 0.1 were obtained for 5 and 15 wt % of HA, respectively. After 3-day washing, these values amounted to 1.23 and 1.59, respectively. Stoichiometric HA ($Ca_5(PO_4)_3OH$) has a theoretical Ca/P ratio of 1.67.

ICP-OES results revealed absence of Ca and P in 0 wt % samples and increasing amounts of Ca and P with

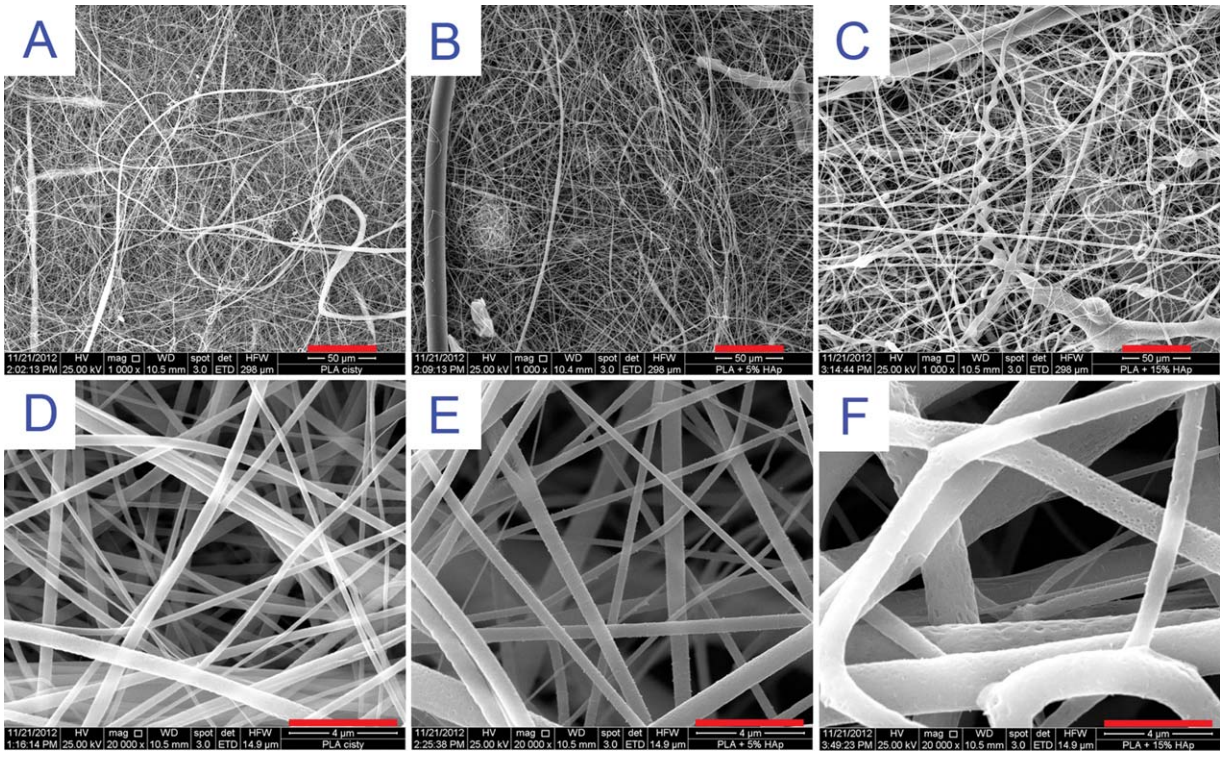

FIGURE 2. SEM micrographs of PLA fibers without HA (A,D), PLA fibers with 5 wt % of HA (B,E) and PLA fibers with 15 wt % of HA (C,F). Bar = 50 μm (A–C) and 4 μm (D–F). [Color figure can be viewed in the online issue, which is available at wileyonlinelibrary.com.]

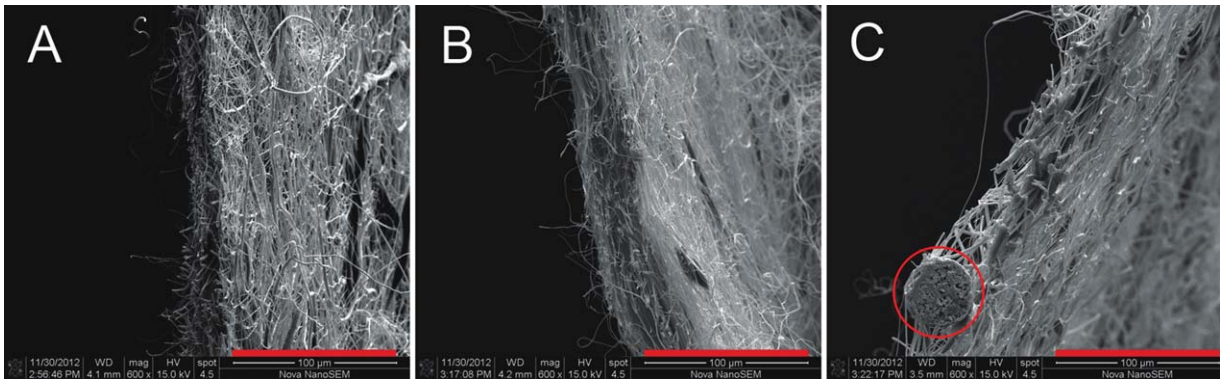

FIGURE 3. Cross sectional SEM images of nanofibers containing 0 wt % of HA (A), 5 wt % of HA (B), and 15 wt % of HA (C). Red circle shows a hydroxyapatite particle in the nanofibrous mat. Bar = 100 μm. [Color figure can be viewed in the online issue, which is available at wileyonlinelibrary.com.]

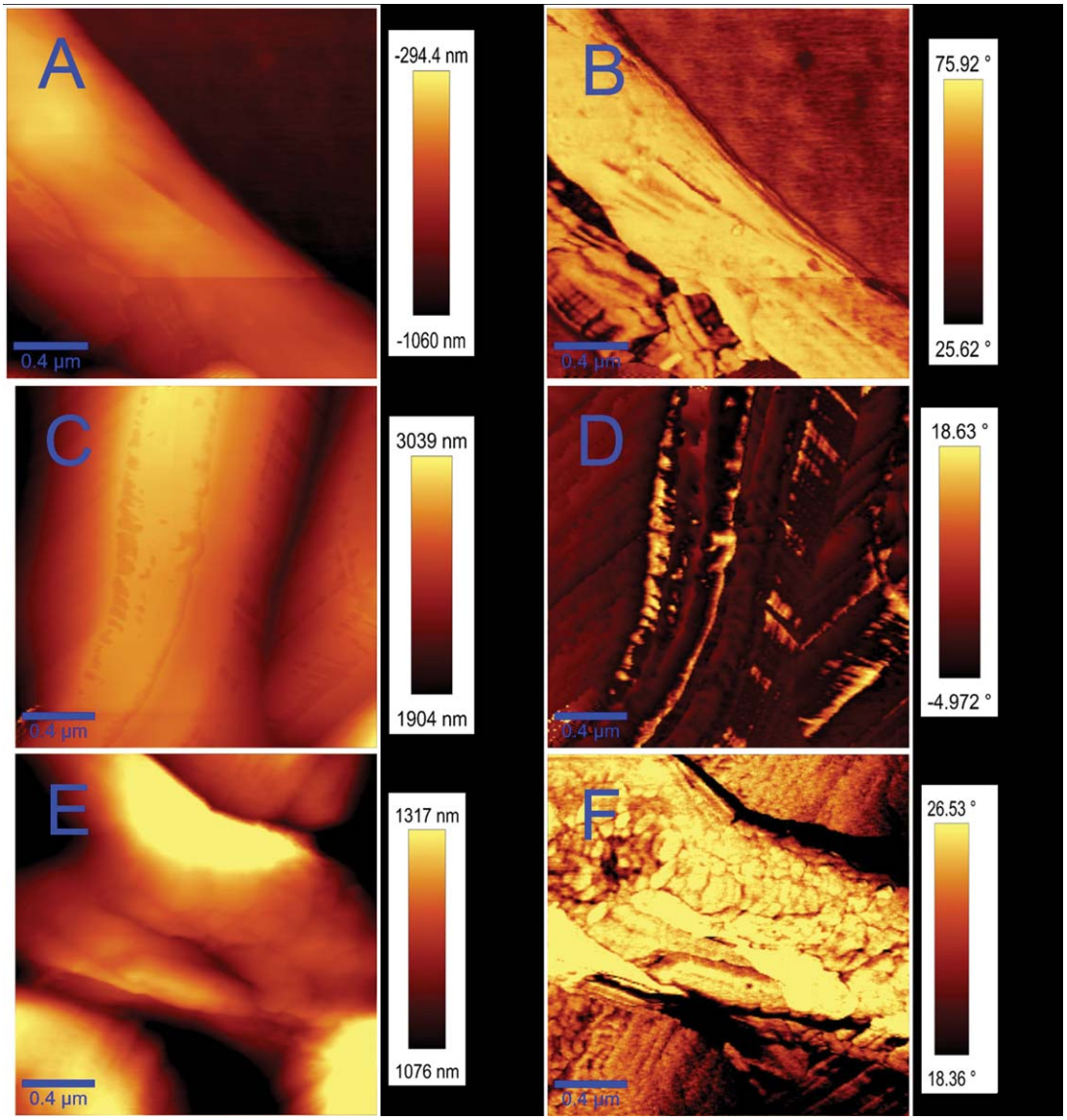

FIGURE 4. AFM images of nanofibers containing 0 wt % of HA (A,B), 5 wt % of HA (C,D) and 15 wt % of HA (E,F). Topographical images (A,C,E), phase images (B,D,F), bar = 0.4 μm. [Color figure can be viewed in the online issue, which is available at wileyonlinelibrary.com.]

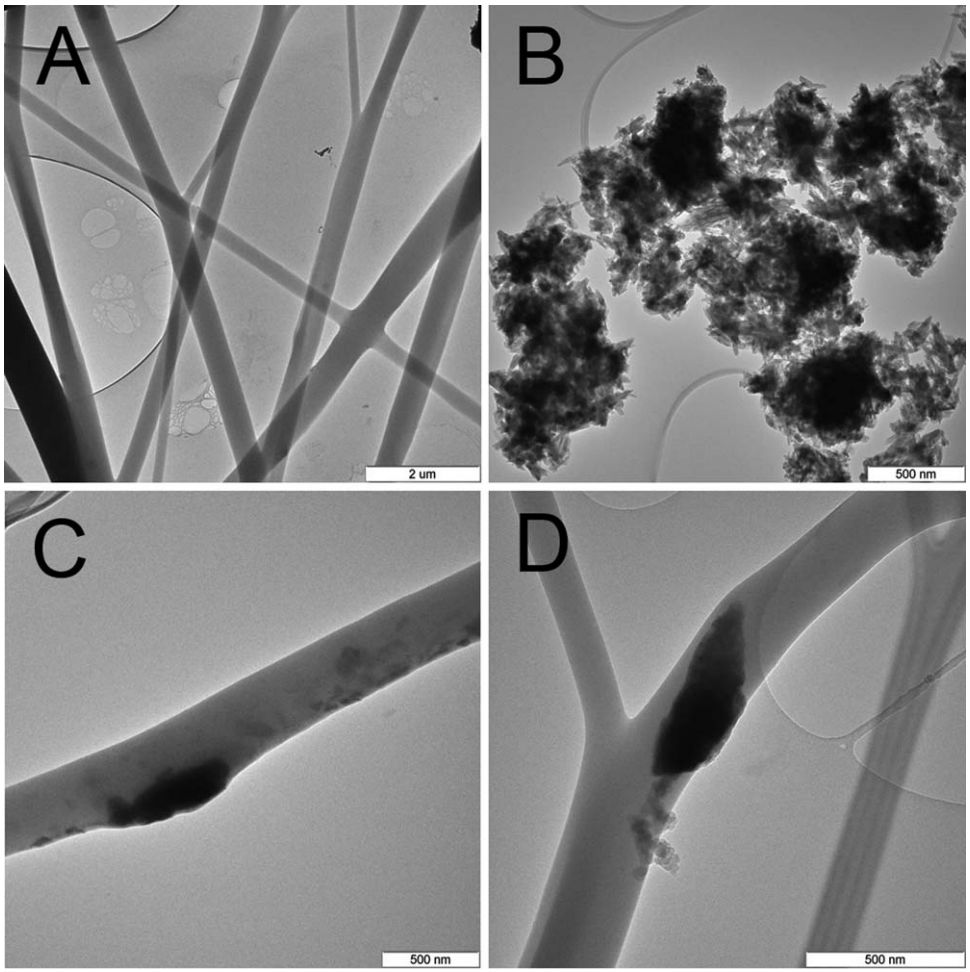

FIGURE 5. TEM images of nanofibers without HA (A), HA nanoparticles (B) and nanofibers with 5 wt % of HA (C) and with 15 wt % of HA (D). The layers with elliptical openings are the amorphous carbon membranes of the grid used to fix the sample. Bar = 2 μm (A) and 500 nm (B–D).

increasing HA content (Table I). The Ca/P ratios detected for 5 and 15 wt % of HA samples were 1.28 and 1.52, respectively. After washing, the Ca/P ratio was measured only in 15 wt % of HA samples, and it was 1.62.

The real content of HA incorporated into PLA measured by TGA was found to be lower than the input contents. In 5 and 15 wt % of HA samples, the real content of HA was 3.1 and 11.4 wt %, respectively. After 3-day washing, the content of HA decreased to 2.1 and 10.5 wt % in 5 and 15 wt % of HA samples, respectively.

As revealed by ATR-FTIR spectroscopy, the most characteristic bands of pure PLA [Fig. 9(A)] include a broad carboxyl O-H related band centered at 3500 cm^{-1}, weak bands in the region 2800–3000 cm^{-1} related to the stretching of CH_2 and CH_3 groups, C=O stretching of ester groups at 1757 cm^{-1}, CH_3 bending at 1455 cm^{-1}, wagging vibrations of CH_2 groups at 1366 and 1383 cm^{-1}, =C–O stretching at 1265, 1130, 1089, and 1047 cm^{-1}, and CH bending vibrations at 871 cm^{-1}. The spectra of PLA with HA [Fig. 9(B,C)] show the increase of CH bands in intensity in comparison with pure nanofibrous PLA.

Mechanical properties of the scaffolds

The mechanical tests showed that dry HA-free PLA samples reached the creep limit rapidly, a small linear elastic region with maximum $3.57 \pm 0.29\%$ elongation and equivalent stiffness 22.82 ± 0.69 mN/mm. Samples remained at this limit of maximum resisted equivalent force (36.2 ± 1.09 mN/mm) without any hardening, which covered a relatively large region of plastic deformation, up to $35.53 \pm 0.61\%$ elongation, until rupture occurred. On the other hand, wet HA-free PLA samples approached the creep limit immediately, after 0.15% elongation with equivalent stiffness 21.13 mN/mm. The maximum resisted equivalent force was 6.75 mN/mm; however, the region of plastic deformation (35% elongation) is similar to that of dry HA-free PLA samples.

The PLA samples with 5 and 15 wt % of HA exhibited similar mechanical behavior. In the dry state, the response was strictly linear, and represented by equivalent stiffness 15.66 ± 0.53 mN/mm for 5 wt % of HA and 13.31 ± 1.19 mN/mm for 15 wt % of HA samples. The samples were ruptured at $3.19 \pm 0.33\%$ elongation ($3.57 \pm 0.21\%$ for 15 wt % of HA), maximum equivalent force 23.35 ± 1.01 mN/mm

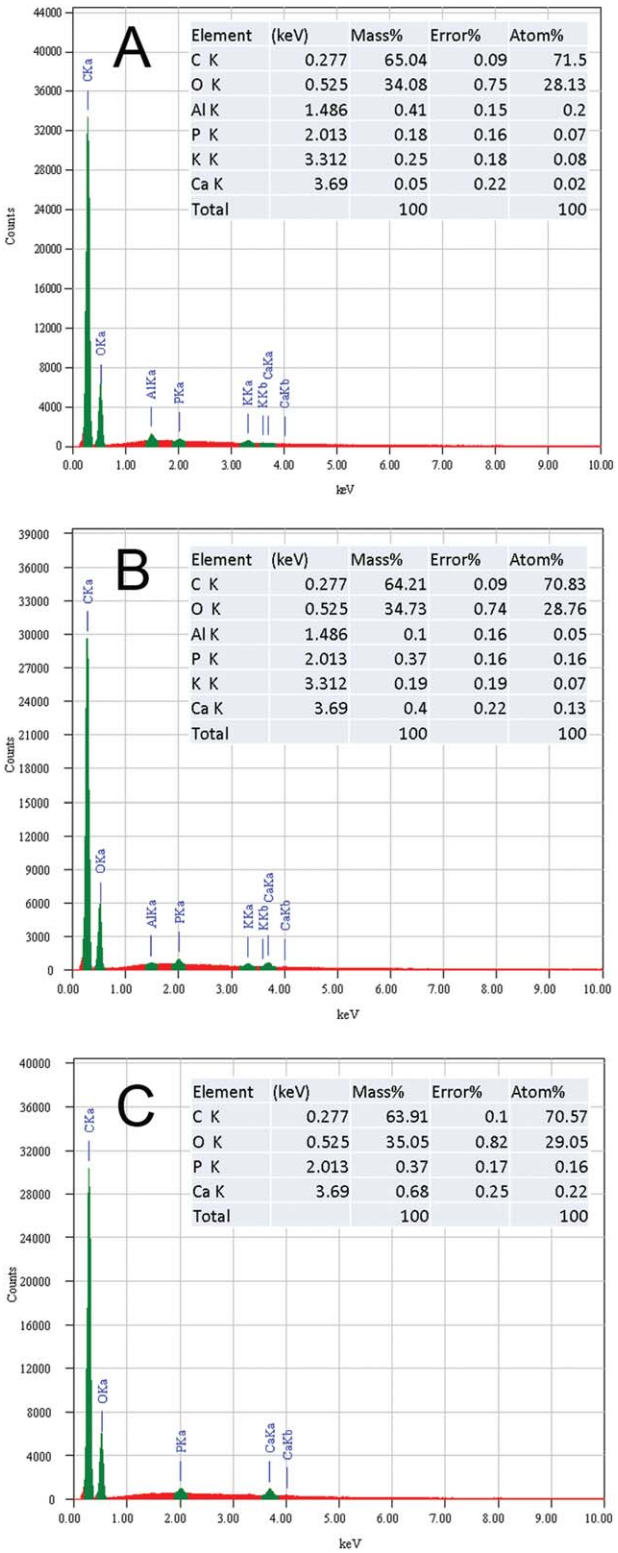

FIGURE 6. EDS spectra and elemental composition of nanofibers containing 0 wt % of HA (A), 5 wt % of HA (B), and 15 wt % of HA (C). [Color figure can be viewed in the online issue, which is available at wileyonlinelibrary.com.]

(20.73 ± 1.45 mN/mm for 15 wt % of HA). In contrast, the wet samples of PLA with 5 wt % of HA and 15 wt % of HA displayed creep behavior. The equivalent stiffness remained at a similar level as for the dry samples (11.27 ± 0.64 mN/mm) but the elastic region was dramatically shortened within the elongation reached ($0.62 \pm 0.23\%$). The rupture occurred at $11.3 \pm 3.26\%$ elongation, maximum equivalent force 2.17 ± 0.98 mN/mm.

Cell growth and viability

On days 1 and 7 after seeding, the number of MG 63 cells was higher on control polystyrene (PS) than on PLA-based samples. Among these samples, however, the cell number was the highest on samples with 15 wt % of HA on day 7 [Fig. 10(A,B)]. The growth curve of cells cultured on the 0 wt % of HA samples had an ascending trend from day 1 to day 3, but from day 3 to day 7 the growth of the cells was more or less stagnant. On the other hand, the situation was reversed on samples with 5 or 15 wt % of HA, where the ascending growth trend was detected between day 3 and day 7 [Fig. 10(C)]. In accordance with these results, XTT test revealed significantly higher quantity of metabolically active cells on the PLA with 15 wt % of HA after 7 days of static cultivation. Similar results were found on samples cultivated under the dynamic conditions. Also, under these conditions, the cell metabolic activity was improved, which was more apparent on nanofibrous samples than on PS (Fig. 11). Live/dead staining on day 7 revealed no considerable cytotoxic effect caused by PLA scaffolds or by HA incorporated into the PLA. Cells created confluent layers on all tested materials on day 7 (Fig. 12).

Osteogenic cell differentiation

The presence of osteocalcin in cells grown on the tested materials was proved by immunofluorescence staining. Osteocalcin was brightly stained, creating typical dot-like structures in the cell cytoplasm (Fig. 13). ELISA revealed a significantly higher concentration of osteocalcin in cells grown on PLA with 15 wt % of HA than in cells on the pure PLA [Fig. 14(A)]. However the concentrations of osteocalcin in cells on the samples with 15 wt % of HA did not reach the values on the control PS.

Potential cell immune activation

Potential immune activation of cells on the tested materials, measured by the levels of TNF-α released into the cell culture media, was relatively low. For the PLA-based materials, these levels ranged between 4.8 and 5.3 pg/100,000 cells, while after LPS treatment of cells, these values amounted to 21 pg/100,000 cells [Fig. 14(B)].

DISCUSSION

It was found that loading the PLA nanofibers with HA changed their morphology, chemical composition and mechanical properties, and increased their ability to support cell colonization and osteogenic cell differentiation.

Measuring the diameter of PLA fibers (Fig. 1) revealed that with increasing HA content, the fibers became thicker and more irregular in shape. Their diameter was, in fact, of submicron size, because the size of nanostructures is defined to be equal to or less than 100 nm.[10] However, in a wide

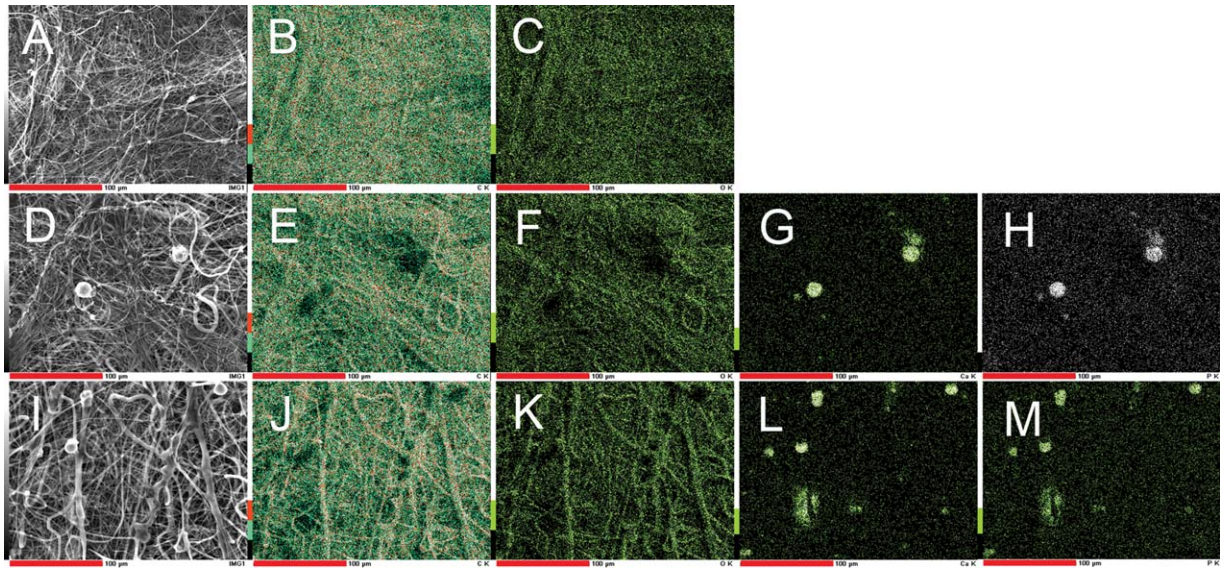

FIGURE 7. SEM and EDS-based elemental mapping images of nanofibers containing 0 wt % of HA (A–C), 5 wt % of HA (D–H) and 15 wt % of HA (I–M). SEM image of area analyzed by EDS mapping (A,D,I), EDS-based elemental mapping images for carbon (B,E,J), oxygen (C,F,K), calcium (G,L), and phosphorus (H,M). Bar = 100 μm. [Color figure can be viewed in the online issue, which is available at wileyonlinelibrary.com.]

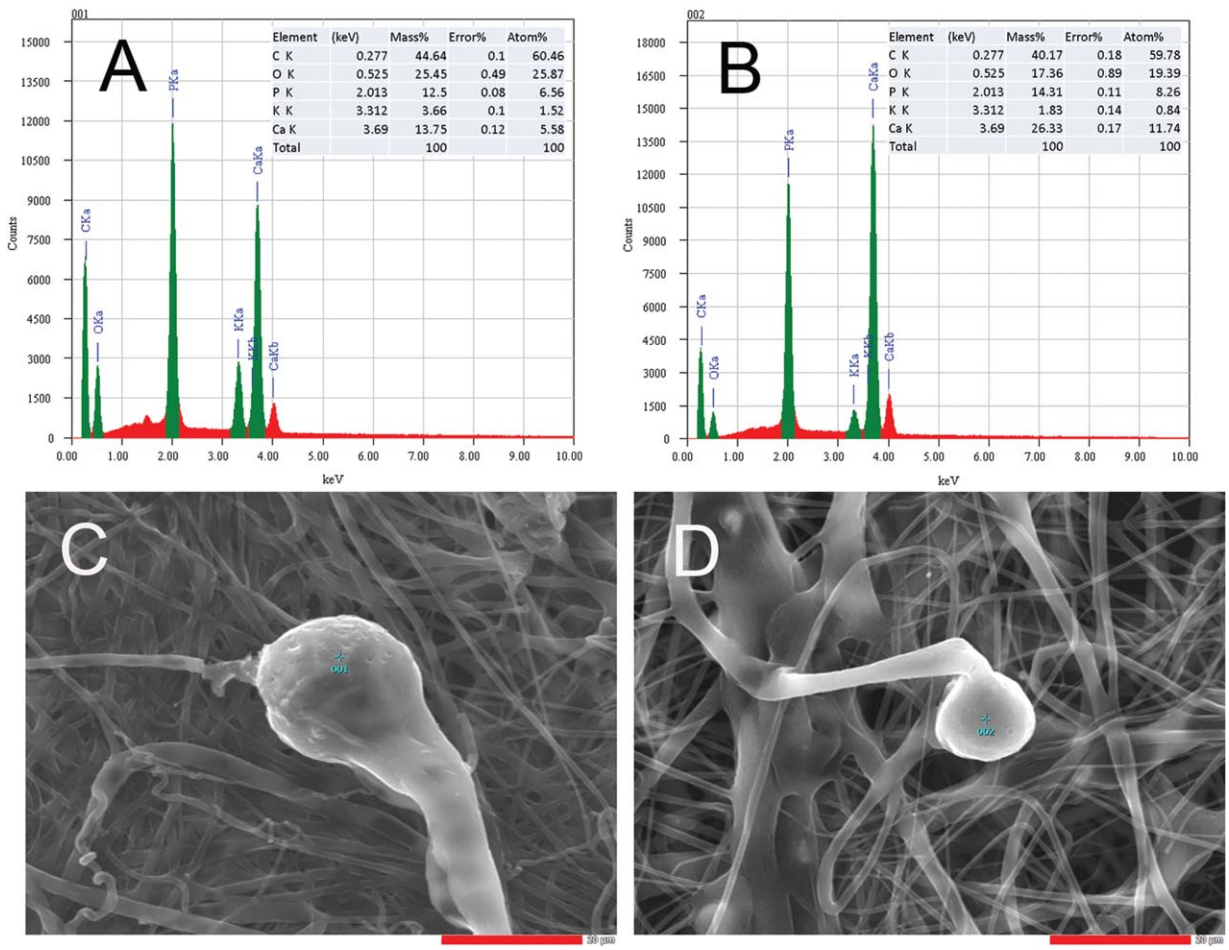

FIGURE 8. SEM-EDS spot analysis of a spherical HA particle in a sample with 5 wt % of HA (A,C) and in a sample with 15 wt % of HA (B,D). EDS spectra and elemental composition (A,B) corresponding to the marked spot on the secondary electron micrograph (C,D). Bar = 20 μm. [Color figure can be viewed in the online issue, which is available at wileyonlinelibrary.com.]

TABLE I. Mass Percentage of Samples Attributable to Elemental Ca and P Calculated from ICP-OES Data

Sample	Mass Percentage Attributable to Element (%)		Ca/P Molar Ratio
	Ca	P	
0% HA	0.10	0.19	0.43
5% HA	1.17	0.71	1.28
15% HA	4.78	2.44	1.52

range of studies, the submicron-scale fibers are commonly referred to as nanofibres.[1,11,12] Also, from the SEM photographs (Fig. 2), it is evident that the fibers with HA, particularly those with 15 wt % of HA, are mostly thicker than the pure PLA fibers. Similar results were obtained in PLGA with 0.5 to 15 wt % of HA, where a tendency for the fiber diameter to increase with the HA content was observed.[12] On the other hand, some authors reported that the fiber diameter decreased with increasing HA concentration, for example, in PLA scaffolds with 5 or 20 wt % of HA[11] or in composite PCL/PLA/HA nanofibrous scaffolds.[4] The decrease of the fiber diameter was explained by a lower viscosity of the polymer solution after addition of HA nanoparticles. The measurement of the thickness of the nanofibrous membranes also showed the enlargement of the fibers with HA incorporation (Fig. 3).

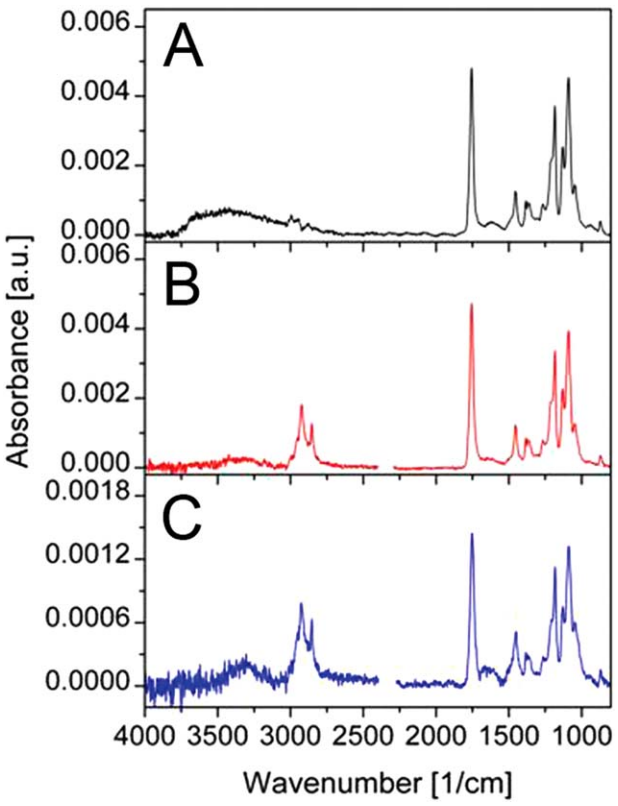

FIGURE 9. Infrared spectra of nanofibers containing 0 wt % of HA (A), 5 wt % of HA (B), and 15 wt % of HA (C). [Color figure can be viewed in the online issue, which is available at wileyonlinelibrary.com.]

AFM and TEM analysis (Figs. 4 and 5) revealed that HA was incorporated quite inhomogeneously throughout the scaffolds and formed clusters. The EDS-based elemental mapping also showed that the most intense signals for Ca and P were observed in spherical regions (Fig. 7). Similar results were also observed in our earlier study performed on PLGA nanofibers loaded with nanodiamond particles.[6] These findings indicate that vortexing and sonication, used in our studies, was probably not fully sufficient to prevent the clustering of nanoparticles. On the other hand, Jeong et al. reported homogeneous distribution of HA nanoparticles exclusively inside poly(L-lactide) (PLLA) fibers without forming lumps on the fibers or between them. This favorable result was attributed to proper adjustment of the parameters during electrospinning, such as the solvent concentration, voltage and infusion speed.[11]

ICP-OES determination of elemental Ca and P contents (Table I) was consistent with EDS results. Before washing, 4.1 and 3.4 times as much Ca and P, respectively, was present in 15 wt % samples compared to 5 wt % samples, and this trend remained similar after washing (see Supporting Information). Three-day washing of the composite membranes in distilled and deionized water generally resulted in minor decreases in Ca and P content and a slight increase in the Ca/P molar ratio. This ratio in the 15 wt % samples (1.52 before and 1.62 after washing) was closer to that of stoichiometric HA (1.67) than that in the 5 wt % of HA group (comparable also with the EDS spot analysis; Fig. 8) and was close to the value typical for so-called calcium-deficient HA (CDHA) which is similar to biological bone apatite. CDHA of Ca/P ratio 1.5 improved viability and alkaline phosphatase activity in MG 63 cells and led to a faster degradation time in comparison with HA of Ca/P ratio 1.67.[8]

TGA revealed that the final contents of HA in PLA were lower than the initial ones. The loss could be due to the sedimentation of HA during the nanofiber preparation. From electrospinning practice, it is known that the incorporation of various bioactive substances, including nanoparticles, into nanofibers is about 75–80% of the substance added to the initial solution. Another explanation could be dissolution of HA by acidic degradation products of PLA. Further moderate loss of HA after 3-day washing of the composite scaffolds in water could be due to dissolution or release of HA particles not firmly attached to the fiber surface.

Analysis of mechanical properties showed that wetting of the samples promoted creep behavior. In the dry state, only PLA without HA showed creep behavior. The PLA with 5 and 15 wt % of HA had only an elastic region and displayed a very fragile response. The increase of HA in the materials caused a decrease of force that is needed for material failure. The results also showed that the elastic reversible region is generally very small, decreasing with the percentage of HA and, with wetting, as much as five times, mostly for HA-containing materials. These results are in accordance with the generally known brittle nature of HA and other ceramics, which limits the use of these materials in load-bearing applications.[11] On the other hand, HA is

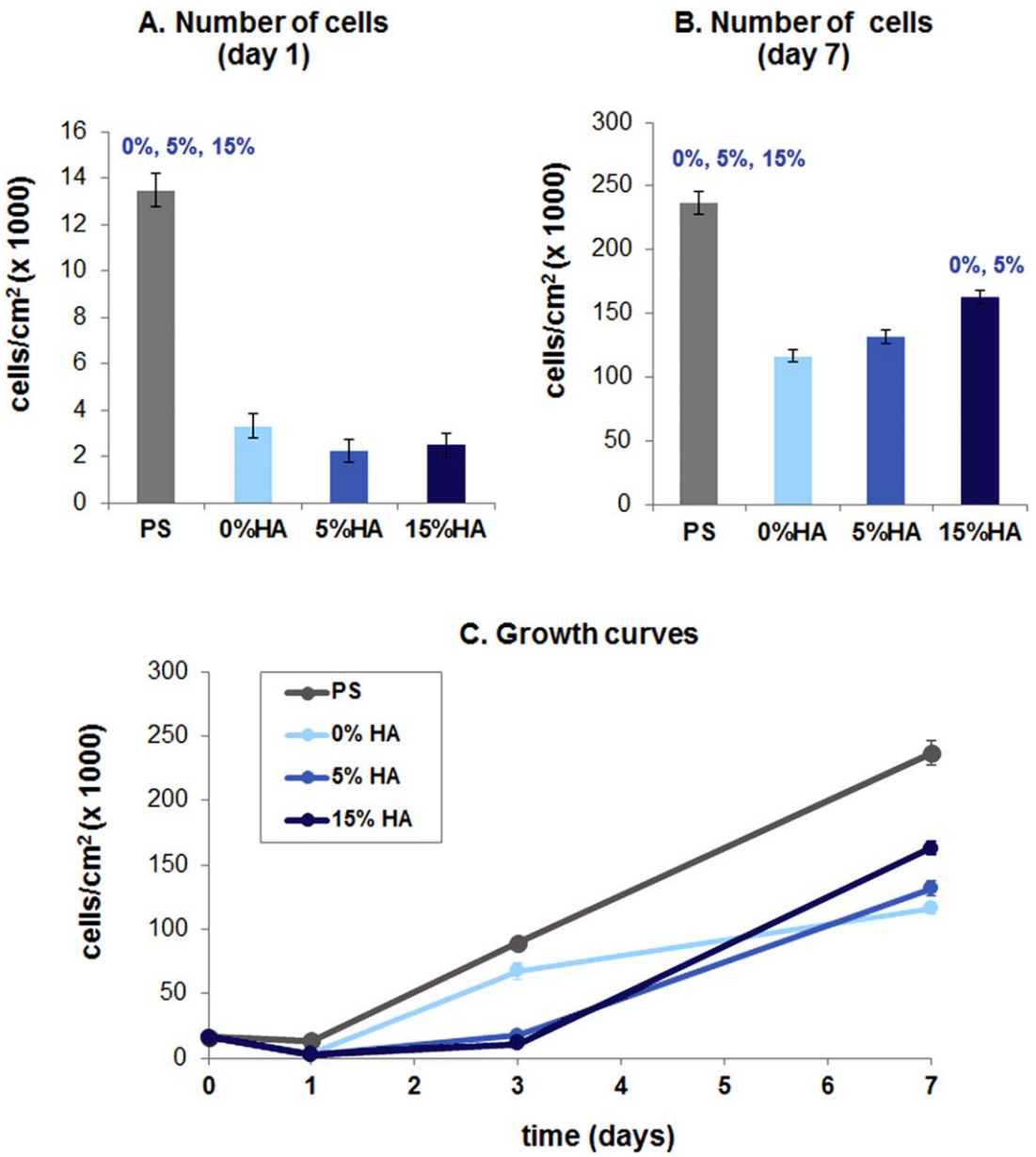

FIGURE 10. Number of human osteoblast-like MG 63 cells on day 1 (A) and day 7 (B) after seeding and growth curves of these cells (C) in cultures on control polystyrene (PS), PLA without hydroxyapatite (0% HA), PLA enriched with 5 wt % of HA (5% HA) and on PLA with 15 wt % of HA (15% HA). Means ± SEM from three samples, each measured two times. ANOVA, Student-Newman-Keuls method. Statistical significance ($p \leq 0.05$) in comparison with other experimental groups is indicated by the names of these groups above the columns. The cell number is given per cm^2 and this area is representative of the surface area. [Color figure can be viewed in the online issue, which is available at wileyonlinelibrary.com.]

commonly believed to reinforce the nanofibrous scaffolds,[4,12] and its addition to PLA nanofibers stabilized their tensile strength, elongation and Young's modulus.[11]

The number of MG 63 cells was higher on control PS than on PLA samples [Fig. 10(A,B)]. This was probably caused by a limited cell–material contact on fibrous scaffolds compared to planar (flat) substrates[6,7] rather than by the material cytotoxicity, because staining with a live/dead kit revealed similar viability of cells on control PS dishes and all nanofibrous scaffolds (Fig. 12). These findings are compatible with a similar study on PLA/HA composites with 5 and 20 wt % of HA, which did not cause any cytotoxicity or considerable inhibition of cell proliferation.[11] Moreover, on day 7, the cell number on our PLA samples was positively correlated with the HA concentration and was highest on samples with 15 wt % of HA [Fig. 10(B)]. This result was further confirmed by results of the XTT test performed under both static and dynamic conditions (Fig. 11). Also in studies by other authors, the enrichment of PLA-based or other polymeric nanofibrous scaffolds with HA stimulated the proliferation of osteogenic cells,[4,13] which can be explained by upregulated expression of genes associated with cell proliferation by HA,[17] direct mitogenic

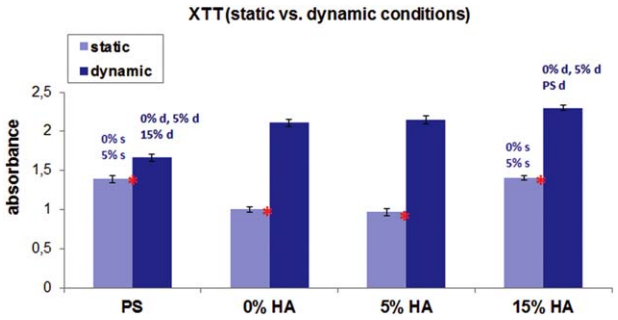

FIGURE 11. XTT assay (cell proliferation kit II) of MG 63 cells on day 7 after seeding on control polystyrene (PS), PLA without hydroxyapatite (0% HA), PLA enriched with 5 wt % of HA (5% HA) or with 15 wt % of HA (15% HA) cultured under static (s) or dynamic (d) conditions. Means ± SEM from three samples, each measured three times. ANOVA, Student-Newman-Keuls Method. Statistical significance ($p \leq 0.05$) in comparison with other experimental groups is indicated by the names of these groups above the columns. Student's *t*-test applied for two experimental groups comparisons. *There is a statistically significant difference for the two (static vs. dynamic) input groups. [Color figure can be viewed in the online issue, which is available at wileyonlinelibrary.com.]

effects of HA crystals,[18] and also by the reinforcement of the material and its functioning as a stronger support for cell colonization.[11,13] The growth curves [Fig. 10(C)] suggest that cell growth on HA-containing scaffolds was slightly delayed, although the final cell population densities increased with increasing HA concentration. Analogical results were found in MC3T3-E1 cells on PLLA scaffolds loaded with 20 wt % of HA. On day 7 after seeding, the cell number on these scaffolds was lower than on pure PLLA scaffolds, but on day 21, on average it became higher.[11]

Cultivation under the dynamic conditions improved overall proliferation of the cells, probably because of the better access of the nutrients and oxygen to the cells, quicker waste removal and also mechanical stimulation of cells. Circular movement of the shaking plate induced flow of the culture medium, and this type of mechanical stimulation has been reported to promote the proliferation of cells.[19]

The osteocalcin analysis suggested that the 15 wt % of incorporated HA had a positive impact on cell differentiation. The amount of Ca and P released from these scaffolds could be higher than from the scaffolds with 5% HA. It is known that dissolution of various biomaterials containing Ca and P, such as HA[20] or silica-calcium phosphate composites[21] increase the osteogenic cell differentiation. Also the addition of Ca ions directly to the culture media stimulated the production of osteocalcin.[20] Another factor promoting the osteogenic cell differentiation could be the hard areas found in the 15 wt % of HA sample by AFM.

Even though no cytotoxicity of the tested scaffolds was observed, there can be some negative impact on the cells, such as cell immune activation, which is calculable for example, by production of TNF-α. TNF-α is a cytokine associated with inflammation and cancer development (for a review, see Ref. 6). In our previous study,[6] almost no response of MG 63 cells to the LPS treatment was observed, even when relatively high concentrations of LPS were

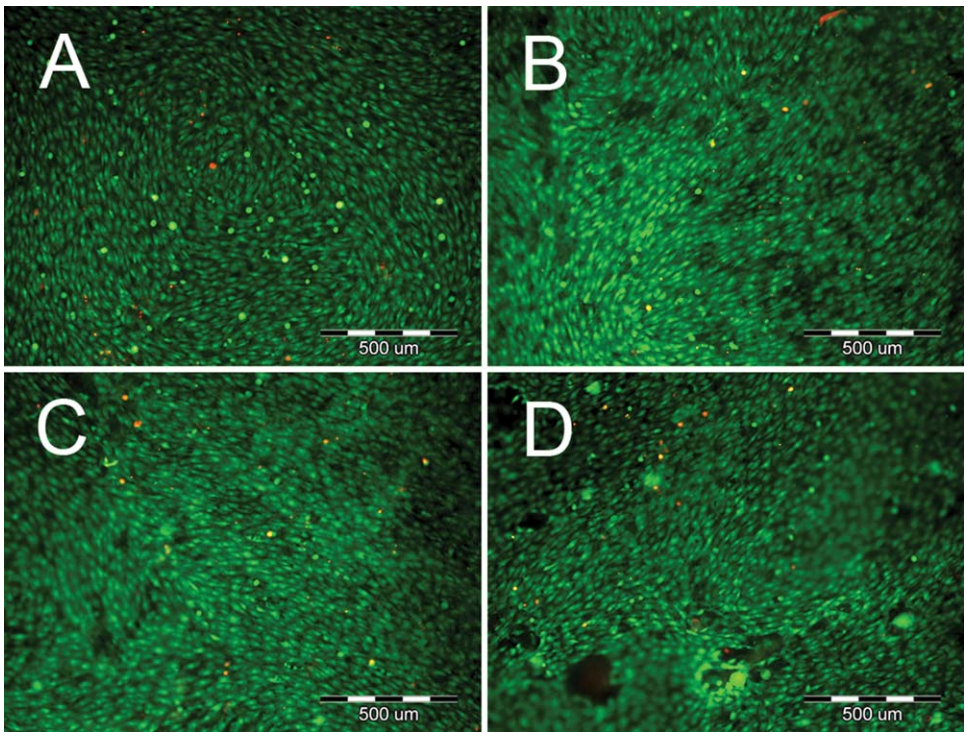

FIGURE 12. Live/dead staining of MG 63 cells on day 7 after seeding on control PS (A), PLA with 0 wt % of HA (B), 5 wt % of HA (C), and with 15 wt % of HA (D). Fluorescence microscope Olympus IX 71, obj. 10×, bar = 500 μm. [Color figure can be viewed in the online issue, which is available at wileyonlinelibrary.com.]

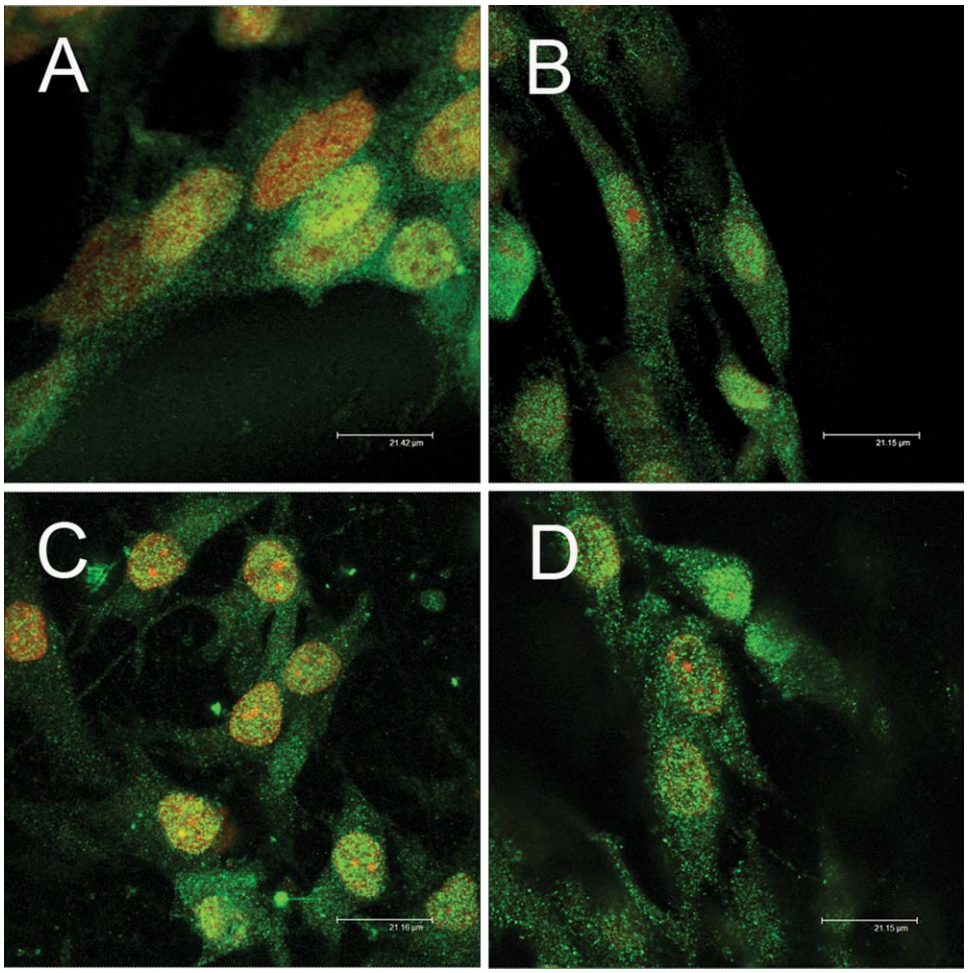

FIGURE 13. Immunofluorescence staining of osteocalcin in MG 63 cells on day 7 after seeding on control PS (A), PLA with 0 wt % of HA (B), 5 wt % of HA (C), and with 15 wt % of HA (D). The cell nuclei were counterstained with propidium iodide. Confocal microscope Leica SP2 AOBS, bar = 21 μm. A: obj. 20×; zoom 7.2×; B–D: obj. 63×; zoom 2.25×. [Color figure can be viewed in the online issue, which is available at wileyonlinelibrary.com.]

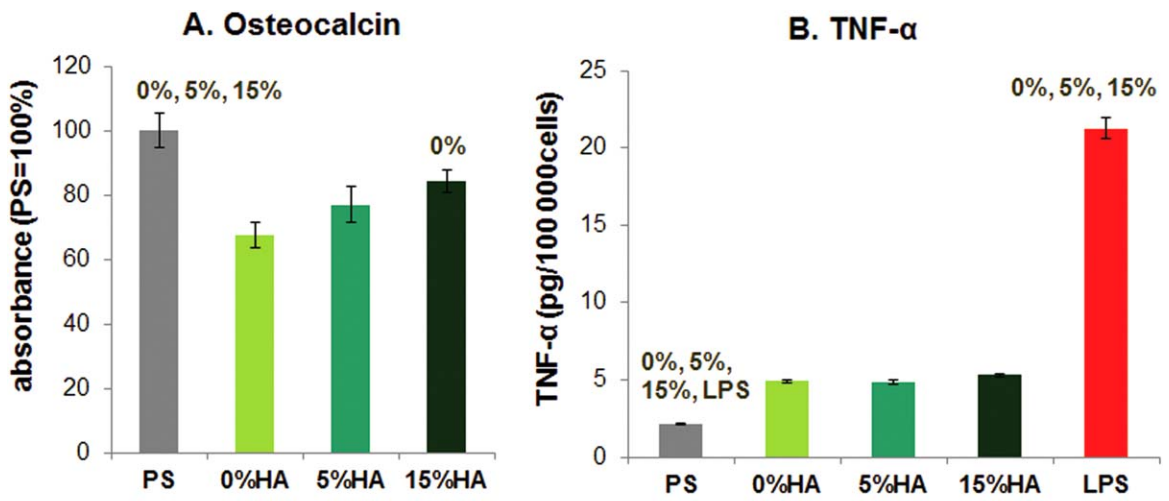

FIGURE 14. Concentration of osteocalcin in MG 63 cells on day 7 after seeding on PLA nanofibrous materials and on control PS. Measured by ELISA per mg of protein, absorbance values were expressed in % of values obtained from cells grown on control PS. Mean ± SEM from six independent samples for each experimental group; each sample measured four times (A). Concentration of tumor necrosis factor-alpha (TNF-α) in culture media taken from RAW 264.7 cells cultured on PLA nanofibrous materials and on control PS for 7 days. Positive control (LPS): Cells after 24-h stimulation with bacterial lipopolysaccharide (0.5 ng/mL) (B). Mean ± SEM from three independent samples for each experimental group (each measured twice). ANOVA, Student-Newman-Keuls method. Statistical significance ($p \leq 0.05$) in comparison with other experimental groups is indicated by the names of these groups above the columns. [Color figure can be viewed in the online issue, which is available at wileyonlinelibrary.com.]

applied (up to 10 μg/mL). Therefore, macrophage-like RAW 264.7 cells were used for the evaluation. A positive response to the LPS stimulation was obtained, even when a low concentration of 0.5 ng/mL of LPS was applied to the cell culture media. No significant increase in TNF-α level was detected in connection with HA incorporation into the PLA.

CONCLUSION

The nanofibrous PLA scaffolds enriched with 5 or 15 wt % of HA provided a good support for the adhesion, growth, and osteogenic differentiation of human osteoblast-like MG 63 cells. At the same time, no significant immune activation of the macrophage-like RAW 264.7 cells cultivated on the tested scaffolds was observed. Thus, these scaffolds are promising as cell carriers for bone tissue engineering, particularly in non-load-bearing applications.

REFERENCES

1. Woo KM, Jun JH, Chen VJ, Seo J, Baek JH, Ryoo HM, Kim GS, Somerman MJ, Ma PX. Nano-fibrous scaffolding promotes osteoblast differentiation and biomineralization. Biomaterials 2007;28: 335–343.
2. Dubsky M, Kubinova S, Sirc J, Voska L, Zajicek R, Zajicová A, Lesny P, Jirkovska A, Michalek J, Munzarova M, Holan V, Sykova E. Nanofibers prepared by needleless electrospinning technology as scaffolds for wound healing. J Mater Sci Mater Med 2012;23:931–941.
3. Jin L, Wang T, Zhu ML, Leach MK, Naim YI, Corey JM, Feng ZQ, Jiang Q. Electrospun fibers and tissue engineering. J Biomed Nanotechnol 2012;8:1–9.
4. Fang R, Zhang E, Xu L, Wei S. Electrospun PCL/PLA/HA based nanofibers as scaffold for osteoblast-like cells. J Nanosci Nanotechnol 2010;10:7747–7751.
5. Yeo M, Lee H, Kim G. Three-dimensional hierarchical composite scaffolds consisting of polycaprolactone, β-tricalcium phosphate, and collagen nanofibers: Fabrication, physical properties, and in vitro cell activity for bone tissue regeneration. Biomacromolecules 2011;12:502–510.
6. Parizek M, Douglas TE, Novotna K, Kromka A, Brady MA, Renzing A, Voss E, Jarosova M, Palatinus L, Tesarek P, Ryparova P, Lisa V, dos Santos AM, Bacakova L. Nanofibrous poly(lactide-*co*-glycolide) membranes loaded with diamond nanoparticles as promising substrates for bone tissue engineering. Int J Nanomed 2012;7: 1931–1951.
7. Okada S, Ito H, Nagai A, Komotori J, Imai H. Adhesion of osteoblast-like cells on nanostructured hydroxyapatite. Acta Biomater 2010;6:591–597.
8. Wang Z, Li M, Yu B, Cao L, Yang Q, Su J. Nanocalcium-deficient hydroxyapatite-poly (e-caprolactone)-polyethylene glycol-poly (e-caprolactone) composite scaffolds. Int J Nanomed 2012;7:3123–3131.
9. Allegrini S Jr, Rumpel E, Kauschke E, Fanghänel J, König B Jr. Hydroxyapatite grafting promotes new bone formation and osseointegration of smooth titanium implants. Ann Anat 2006; 188:143–151.
10. Murugan R, Ramakrishna S. Development of cell-responsive nanophase hydroxyapatite for tissue engineering. Am J Biochem Biotechnol 2007;3:118–124.
11. Jeong SI, Ko EK, Yum J, Jung CH, Lee YM, Shin H. Nanofibrous poly(lactic acid)/hydroxyapatite composite scaffolds for guided tissue regeneration. Macromol Biosci 2008;8:328–338.
12. Lao L, Wang Y, Zhu Y, Zhang Y, Gao C. Poly(lactide-co-glycolide)/hydroxyapatite nanofibrous scaffolds fabricated by electrospinning for bone tissue engineering. J Mater Sci Mater Med 2011;22: 1873–1884.
13. Song W, Markel DC, Wang S, Shi T, Mao G, Ren W. Electrospun polyvinyl alcohol-collagen-hydroxyapatite nanofibers: A biomimetic extracellular matrix for osteoblastic cells. Nanotechnology 2012;23:115101.
14. Kubies D, Rypacek F, Kovarova J, Lednicky F. Microdomain structure in polylactide-block-poly(ethylene oxide) copolymer films. Biomaterials 2000;21:529–535.
15. Douglas TE, Messersmith PB, Chasan S, Mikos AG, de Mulder EL, Dickson G, Schaubroeck D, Balcaen L, Vanhaecke F, Dubruel P, Jansen JA, Leeuwenburgh SC. Enzymatic mineralization of hydrogels for bone tissue engineering by incorporation of alkaline phosphatase. Macromol Biosci 2012;12:1077–1089.
16. Vandrovcova M, Hanus J, Drabik M, Kylian O, Biederman H, Lisa V, Bacakova L. Effect of different surface nanoroughness of titanium dioxide films on the growth of human osteoblast-like MG63 cells. J Biomed Mater Res A 2012;100:1016–1032.
17. Bombonato-Prado KF, Bellesini LS, Junta CM, Marques MM, Passos GA, Rosa AL. Microarray-based gene expression analysis of human osteoblasts in response to different biomaterials. J Biomed Mater Res A 2009;88:401–408.
18. Cooke MM, McCarthy GM, Sallis JD, Morgan MP. Phosphocitrate inhibits calcium hydroxyapatite induced mitogenesis and upregulation of matrix metalloproteinase-1, interleukin-1beta and cyclooxygenase-2 mRNA in human breast cancer cell lines. Breast Cancer Res Treat 2003;79:253–263.
19. Kapur S, Chen ST, Baylink DJ, Lau KH. Extracellular signal-regulated kinase-1 and −2 are both essential for the shear stress-induced human osteoblast proliferation. Bone 2004;35:525–534.
20. Ma S, Yang Y, Carnes DL, Kim K, Park S, Oh SH, Ong JL. Effects of dissolved calcium and phosphorous on osteoblast responses. J Oral Implantol 2005;31:61–67.
21. Gupta G, Kirakodu S, El-Ghannam A. Effects of exogenous phosphorus and silicon on osteoblast differentiation at the interface with bioactive ceramics. J Biomed Mater Res A 2010;95:882–890.